

Investigation of Physical, Mechanical Properties and Long-Term Creep Behavior of Wengé Wood (WW)

Njankouo Jacques Michel¹, Atchounga Kuida Prisca^{2,*}, Foadieng Emmanuel³, Kamdjo Grégoire⁴, Talla Pierre Kisito²

¹Wood Engineering Department, Higher Technical Teacher Training College (HTTTC), University of Yaoundé I, Ebolowa, Cameroon

²Physics Department, University of Dschang, Mechanics and Modeling of Physical Systems Research Unit (UR-2MSP), Dschang, Cameroon

³Civil Engineering Department, Higher Technical Teacher Training College (HTTTC), University of Buéa, Kumba, Cameroon

⁴Civil Engineering Department, Fotso Victor Institute of Technology (IUT-FV), University of Dschang, Bandjoun, Cameroon

Email address:

patchoungakuida@yahoo.com (A. K. Prisca)

*Corresponding author

To cite this article:

Njankouo Jacques Michel, Atchounga Kuida Prisca, Foadieng Emmanuel, Kamdjo Grégoire, Talla Pierre Kisito. Investigation of Physical, Mechanical Properties and Long-Term Creep Behavior of Wengé Wood (WW). *Applied Engineering*. Vol. 4, No. 2, 2020, pp. 27-34.

doi: 10.11648/j.ae.20200402.11

Received: May 22, 2020; **Accepted:** June 8, 2020; **Published:** June 16, 2020

Abstract: In this research work aiming at determining the physical and mechanical properties of the wood species Wengé, attention has also been paid to its creep behavior through an accelerated test technic. It came out from experimental studies that Wengé wood exhibits good dimensional stability parameters and good mechanical characteristics. Meanwhile, classical creep tests are both time consuming and cost intensive because of their long test time. Hence accelerated creep tests are used to extrapolate the information to the time scale of conventional tests on measurements conducted for much shorter durations. In this research work, we also demonstrate the use of stepped isostress method (SSM) in 4-point bending mode as a means of accelerated creep measurement of the wood species *Millettia Laurentii* called Wengé. The SSM employs a load-stepping approach, typically with at least three steps for a single specimen. The tests have been carried out at temperature of 23°C and 65% relative humidity. The flexural properties of the wood were determined. The master curve obtained can be used for predicting the creep behavior of the test material for time periods more exceeding the experimental one. Besides, from the Eyring theory on creep we calculated the activation volume of the *Millettia Laurentii* wood. Of course these findings clearly indicate that the reduction modulus of the wood species *Millettia Laurentii* in this work is increasing over time but at a decreasing rate.

Keywords: Wood, *Millettia Laurentii*, Creep, Activation Volume, Stepped Isostress Method, Four-point Bending Test

1. Introduction

The Wengé wood is one of the oldest building materials used by humans in the south region of Cameroon and in many sub-Saharan African countries. This wood, often overexploited, is used as building materials, insulation, decoration and the manufacture of art objects [1]. Investigations lead to the conclusion that there is unfortunately no study on the determination of its physical and mechanical properties. In addition, the production and uses of Wengé wood are based solely on ancestral ability. This wood offers a real opportunity to the poor local population, to build the houses with that cheap and abundant

material that can meet the need of economic housing. Some information on the basic properties of Wengé wood has been examined [2], but the study of its physico-mechanical properties and applications as raw material is very limited. Further studies are needed to assist and promote its application in the modern world. The optimization of the properties of Wengé wood with a view to its valorization requires knowledge of its mechanical properties through tests such as near infrared spectroscopy [3], static-bending method, longitudinal and complex vibration tests [4] used on some tropical woods. In the same vein creep behavior of this wood should be studied in order to have an idea about its load bearing capacity.

Creep is among the fundamental properties of materials which limiting their long-term application due to excessive deformation or reduced stiffness over an extended period of time [5]. For material design related to the load-bearing capacity of products, the evaluation of creep behavior is indispensable in engineering applications. However, very little attention has been paid to the creep behavior of hardwood. At realistic service-life durations, time is too limited for conducting conventional creep tests, i.e., accelerated tests are necessary [6]. The concept of the accelerated creep test for the prediction of long-term performance is the use of the superposition principle from the combination of exposure time, exposure temperature, and applied load. In other words, a short-term accelerated creep test must be used to obtain the master curve, which is then fitted with an empirical mathematical model. Based on the time-temperature stress superposition principle (TTSSP), the creep behavior of viscoelastic materials can be determined from the stepped temperature and stress in the same manner as time-equivalence [7]. From this principle, the stepped isothermal method (SIM) has been developed to use stepped increments of temperature for a single sample [8–11]. Recently, the stepped isostress method (SSM), which can capture the creep behavior of a single sample with a stepwise increase in the stress level, was successfully applied to semi-crystalline thermoplastics and a carbon-fiber-reinforced polymer [6, 12–14]. In comparison to SIM, additionally, the SSM is more advantageous in evaluating creep behavior of wood, because wood is a low-thermal-conductivity material. However, there is little information available on the SSM method characterizing creep deformation and predicting long-term creep behavior of wood.

2. Materials and Methods

2.1. Determination of Physical and Mechanical Characteristics of WW

The major physical properties we determined in this study are: moisture content (H), density (ρ), volumic shrinkage (R_v) with volumic shrinkage coefficient (r_v), radial shrinkage (R_R) with radial shrinkage coefficient (r_r), tangential shrinkage (R_T) with tangential shrinkage coefficient (r_t), volumic swelling (G_v) with volumic swelling coefficient (g_v), radial swelling (G_R) with radial swelling coefficient (g_r), tangential swelling (G_T) with tangential swelling coefficient (g_t). As far as mechanical properties are concerned, we determined: Young modulus in the direction parallel to fibers, maximum failure stress in compression parallel to fibers ($\sigma_{c//}$) and maximum failure stress in four point bending test perpendicular to fibers ($\sigma_{F\perp}$). Any mentioned characteristic was determined from a sample of 25 specimens of wood (extracted from five different mature billets of *Millettia Laurentii* wood, originating from Kyé-Ossi natural forest in Cameroon south region.) after which we considered the mean value and the standard deviation (S. D.). This was to guarantee the repeatability of each value since wood is an

anisotropic and heterogeneous material. The advantage of considering five different mature billets is that the results would be deemed more representative of the species. Moisture content (H), density (ρ), volumic shrinkage (R_v) with volumic shrinkage coefficient (r_v) and volumic swelling (G_v) with volumic swelling coefficient (g_v) were determined from 25 Wengé wood (WW) specimens of $20 \times 20 \times 20 \text{ mm}^3$ (Figure 1).



Figure 1. WW specimens of $20 \times 20 \times 20 \text{ mm}^3$.



Figure 2. WW specimens of $360 \times 20 \times 20 \text{ mm}^3$.



Figure 3. WW specimens of $60 \times 20 \times 20 \text{ mm}^3$.



Figure 4. WW specimens of $50 \times 50 \times 10 \text{ mm}^3$.

Radial shrinkage (R_R) with radial shrinkage coefficient (r_r), tangential shrinkage (R_T) with tangential shrinkage coefficient (r_t) and radial swelling (G_R) with radial swelling coefficient (g_r), tangential swelling (G_T) with tangential swelling coefficient (g_t) were determined from 25 WW specimens of $50 \times 50 \times 10 \text{ mm}^3$ (Figure 4). Young modulus and σ_{F-L} were determined from WW specimens of $360 \times 20 \times 20 \text{ mm}^3$ (Figure 2) whereas WW specimens of $60 \times 20 \times 20 \text{ mm}^3$ (Figure 3) were used to determine $\sigma_{c//}$. All the 25 wood specimens were tested following the French Norm NF B 51-003 that labels general requirements for physical and mechanical tests. The maximum stress in compression parallel to fibers ($\sigma_{c//}$) has been determined by the means of the compression testing machine (Figure 5).

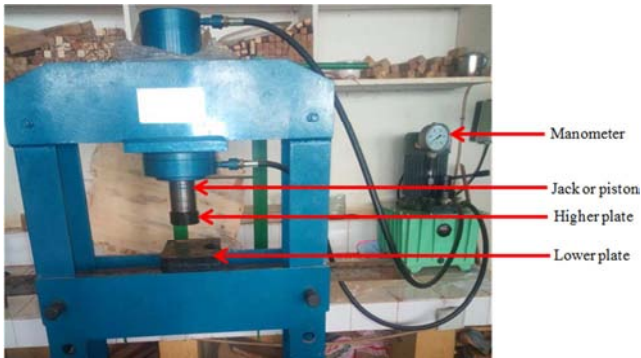


Figure 5. Compression testing machine.

2.2. SSM Creep Tests

The creep tests were conducted at Dschang University (Cameroon) using a four-points flexural test machine (Figure 9) coupled with a strain-bridge (Figure 6) possessing a high accuracy. The indoor temperature was 23°C and the relative humidity was 65% during all the process. The specimens were prepared with a required dimension of $20\text{mm} \times 20\text{mm} \times 360 \text{ mm}$ (Figure 2). During creep test we used strain gauges (Figure 7) having an electric resistance of $R \pm \Delta R$. A strain gauge is made of a threadlike conductor of resistivity ρ , of section S and of length nl ; n stands for the number of strands and l is the length of one strand. The two strain gauges stuck longitudinally on the sample (Figure 8) and symmetrically undergo the same deformation than the wood sample (under the applied load) which the expression is $\frac{\Delta l}{l}$. Since the expression of the resistance of the gauge is:

$$R = \frac{\rho nl}{S} \quad (1)$$

Under the influence of the preceding deformation $\frac{\Delta l}{l}$ this electric resistance varies by ΔR such that

$$\frac{\Delta R}{R} = \frac{\Delta l}{l} + \frac{\Delta \rho}{\rho} - \frac{\Delta S}{S} \quad (2)$$

As $\frac{\Delta \rho}{\rho}$ and $\frac{\Delta S}{S}$ can be set in terms of $\frac{\Delta l}{l}$, the final expression of $\frac{\Delta R}{R}$ is:

$$\frac{\Delta R}{R} = K \frac{\Delta l}{l} \quad (3)$$

Where the value of the gauge factor K is 2.

The strain bridge (Figure 6) converts automatically this relative variation of electric resistance or deformation into a numeric value that we can record.



Figure 6. Numerical strain bridge.

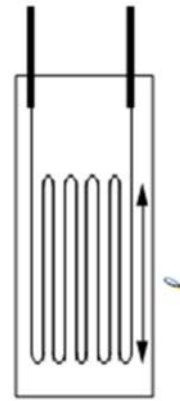


Figure 7. Strain gauge.

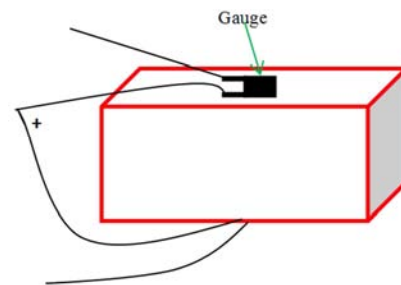


Figure 8. Test specimen carrying two gauges.

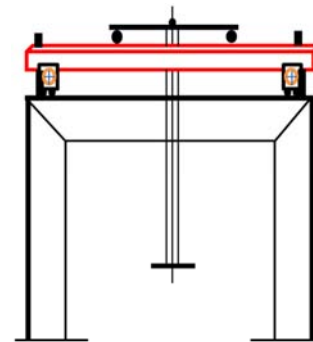


Figure 9. Experiment set-up for creep test.

WW in this paper was studied using SSM at one starting stress level (reference stress), which would be equivalent to the constant sustained stress level during a conventional (long-term) creep test. In this work, since the creep was nondestructive test, the initial stress level and the stress level increment have been chosen in such a way to stay in the domain of lower loads, that would preserve the material from any possible damage. The specimen starts at the reference stress in the first load step, then moves to higher stress levels

with each load step until the final step. These stresses (referred to as accelerating stresses) are expressed in terms of the average failure stress (AFS), meaning reference stress of 5,34% AFS. The accelerating stresses were simply divided into equal stress increments of 4,96 MPa (3,21% AFS), each lasting 3 hours (this step duration was sufficient to appreciate primary and secondary creeps). Table 1 summarizes the test parameters selected for the experiments in this study.

Table 1. Procedure for creep testing WW with the SSM.

Reference stress	Step parameters	Load step					
		1	2	3	4	5	6
5,34% AFS	Stress level (% AFS)	5,34	8,55	11,76	14,97	18,18	21,39
	Step duration (hrs)	3	3	3	3	3	3

AFS: Average Failure Stress; WW: Wengé Wood.

3. Results and Discussion

3.1. Major Physical and Mechanical Characteristics of WW

The degradation of wood products is to dimensional variations linked to shrinkage or swelling. The daily resulting inconveniences can be outlined; doors and windows are locked with difficulty, relative movement in joints, wedging of drawers etc. Parameters of dimensional stability of WW are summarized in the following table 2.

Table 2. Physical characteristics of WW for a moisture content 12%.

Physical properties	Mean value	S. D
ρ_H (g/cm ³)	0,789	0,019
R_v (%)	14,7	0,6
r_v (%)	0,64	0,02
R_R (%)	5,6	0,1
r_r (%)	0,24	0,005
R_T (%)	8,9	0,1
r_t (%)	0,38	0,06
G_v (%)	17,2	0,8
g_v (%)	0,74	0,03
G_R (%)	5,9	0,1
g_r (%)	0,25	0,005
G_T (%)	9,7	0,1
g_t (%)	0,41	0,006

In this table density is reported as mass divided by volume with both at 12% moisture content. The use of WW by engineers and others inspired the study of certain dimensional stability parameters of this wood species (Table 2). The evaluation has been done on three total shrinkages (i.e. volumic, radial and tangential) resulting in water variation in wood fibers. This led us to measure the fibers saturation point (FSP). We didn't determine the longitudinal shrinkage since its value is commonly negligible as compared to values in radial and tangential directions.

Table 3. Mechanical characteristics of WW for a moisture content 12%.

Mechanical characteristics	Mean value	S. D
E_L (MPa)	21058	697,69
σ_{\parallel} (MPa)	78,5	7,2
σ_{\perp} (MPa)	154,6	16,3

The longitudinal direction is the most relevant among the three anisotropic directions of a wood since it is the one that makes it a good structural material. This is why we determined the Young's modulus only in this direction. From these tables, it is straightforward that we are dealing with a heavy wood with high longitudinal Young's modulus. Besides, the shrinkage and the swelling of this wood species are such that its exterior application in wooden structures could be considered.

We determined the fiber saturation point (FSP) of WW through the experimental curve of volumic shrinkage (R_v) vs moisture content (MC). The specimens have been first naturally dried until anhydrous state, then wetted progressively and the volume was determined during the process.

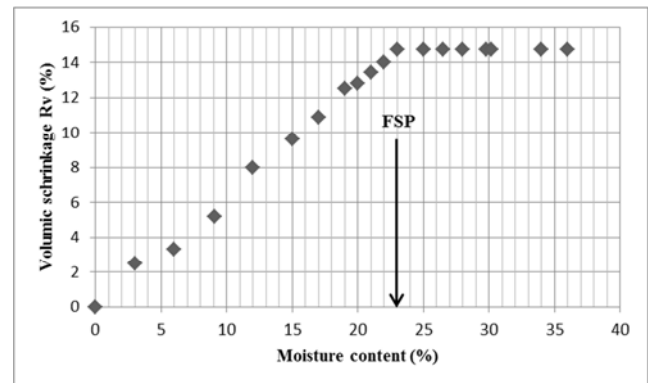


Figure 10. Volumic shrinkage vs moisture content.

Relations between shrinkage and humidity are linear for $0 < MC < FSP$. Moreover when cellular walls are saturated, the colonization of lumens by free water doesn't cause any deformation that is for $MC > FSP$, wood dimensions and volume are constant. The fiber saturation point is the amount of humidity from which the wood volume no more evolves. From Figure 10, it comes that WW doesn't increase volume after 23% of moisture content which is its fiber saturation point.

3.2. Long Term Creep Behavior of WW via SSM

3.2.1. Preliminary Flexural Tests

Before performing the primary experiment, flexural tests were performed with 25 specimens to find the average failure flexural stress of the WW. Specimens measuring approximately 360 mm in length with a squared section of 20 mm in width were prepared. The samples were loaded at a constant strain-rate until complete failure occurred. The average failure flexural stress was 154,6 MPa with a standard deviation of 16,3 MPa. The average elastic modulus, measured in the linear elastic region, was 21058 MPa.

As this work is almost one of the first applying SSM to hardwood, our purpose was to show how this accelerated method works when applying to WW wood. So, we limited ourselves to lower creep stress levels in the experiments. Our maximum creep stress level applied to the sample during SSM creep test was 33,07 MPa representing 21,39% AFS; this was to avoid failure of the specimen and to assure that we remained in the linear region (Figure 11).

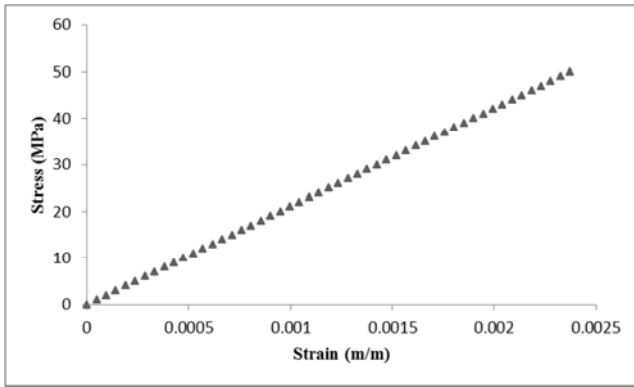


Figure 11. Stress-strain curve for four-point flexural test of WW.

3.2.2. SSM Main Results

For the purpose of this paper, ten specimens were tested for the reference stress at room temperature (23°C) to observe the overall trends in behavior, and to take into account the variability of the wood material. Total strain $\varepsilon_{total}(t)$ is defined as the combination of elastic ε_0 and creep or delayed deformation $\varepsilon_{creep}(t)$ (equation 4), assuming thermal strains are negligible and reference stress is in the elastic region with modulus E_L :

$$\varepsilon_{total}(t) = \varepsilon_0 + \varepsilon_{creep}(t) \quad (4)$$

$$\sigma_0 = \varepsilon_0 \times E_L \quad (5)$$

In equation 5, σ_0 stands for the initial applied stress, ε_0 is the resulting deformation in the elastic region and E_L is the elastic modulus in this elastic linear region.

The stress profile and raw strain data for the SSM creep test are shown in Figure 12 (a) and 12 (b), respectively. Figure 13 contains each step of the data analysis process for 5,34% AFS as an example. There are three major parts of the sequence for analyzing data obtain through the SSM and constructing the creep master curve: (1) vertical shifting, (2)

rescaling, and (3) horizontal shifting.

(1) Vertical shifting is merely the subtraction of elastic strains for each load step to create a continuous curve in terms of strain, as in Figure 13 (a).

(2) Rescaling is the second step, and it essentially accounts for stress history-creep from previous steps-and strain equivalence for each load step, as seen in Figure 13 (b). The method described in [13] is fairly arbitrary and a purely graphical approach is recommended, while the authors in [6] simply recommend fitting a power-law to the secondary creep portions of each stress step for a given sample. In this study, the secondary creep segment for an individual step is extrapolated to zero creep strain ($\varepsilon(t)=0$) using a fractional derivative Maxwell model [2] approximation (Equation 6) (see [2] for the figure of the fractional derivative Maxwell model and the derivation of Equation 6). The secondary creep region was defined from the time point when the creep strain rate varies by less than 0,025% from the start of the load step (i.e., approximately steady-state). The curve is then shifted on the \log_{10} (time) axis by the difference between the real and extrapolated start times of that step, using the following equations:

$$\left\{ \varepsilon(t)_i = \left[\frac{\sigma}{E} + \sum_{k=1}^n \frac{\sigma}{\eta^{\alpha_k}} \frac{(t-t_{k-1})^{\alpha_k}}{\Gamma(1+\alpha_k)} \right]_i \right. \quad (6)$$

$$\left. 0 \leq \alpha_k \leq 1; t_{k-1} \leq t < t_k \right.$$

$$(t_{rescale})_i = (t_{actual})_i - (t_{extrapolated})_i \quad (7)$$

where $i=1, 2, 3...m$ are load steps in the SSM creep test; Γ stands for the gamma function, k is the time step, α_k the power of the fractional derivative model, E the rigidity of the spring, η^{ak} is the viscosity of the spring-pot and σ the applied stress (see [2] for the methodology of determination of the model parameters). The main advantage of the fractional derivative model being that the memory effect of the material is taking into account here and it achieves good fit for rescaling. The creep curve for each load step should be shifted to start at the extrapolated start time, using the rescaling factor $\log_{10}(a_{res})$.

This rescaling procedure for addressing stress history within a sample comes from Schapery's single-integral nonlinear superposition approach, which provides a method for relating strain accumulations at different stress levels and points in time, when the cumulative elastic and creep strains are dependent on stress [13-15].

(3) Finally, the rescaled individual creep curves must be placed along the \log_{10} (time) axis to create the complete master curve, i.e., superposition as in Figure 13 (c). This is accomplished through a shift factor for reduced time, $\log_{10}(a_0)$, and one must be found for each stress level. The result of rescaling is a series of curves, each of which represents part of a creep curve that would have been obtained from tests on different specimens at different stresses. They are thus the same as those that could have been obtained from

separate time stress superposition principle (TSSP) tests. They must be shifted along the logarithmic time axis to obtain the creep master curve at a reference stress. The magnitude of this horizontal shift is a function of stress and is similar in principle to the shift in time temperature superposition principle (TTSP) testing where tests are carried out at different temperatures and the shift is a function of temperature.

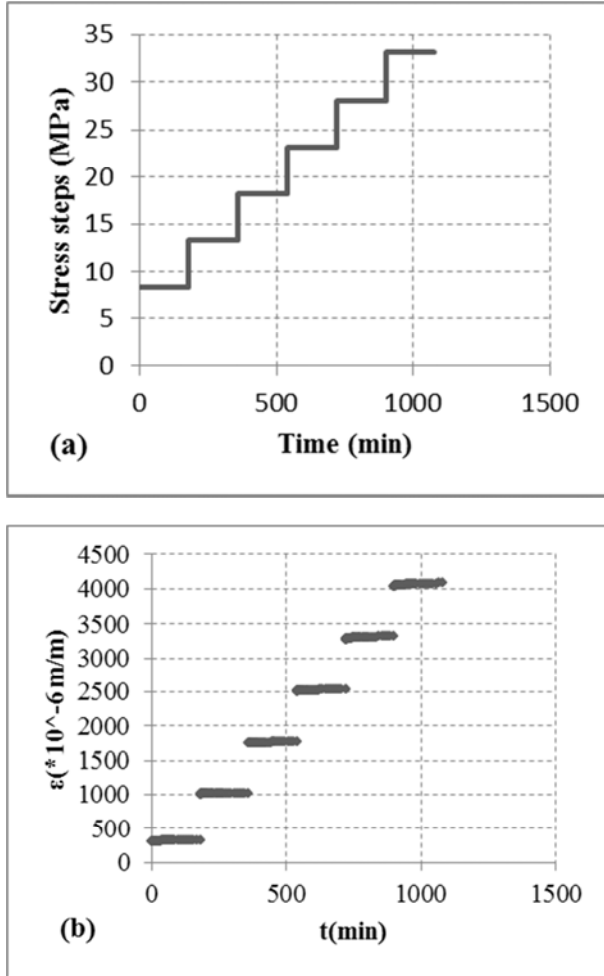


Figure 12. SSM creep test results: (a) Stress profile, and (b) Raw strain data.

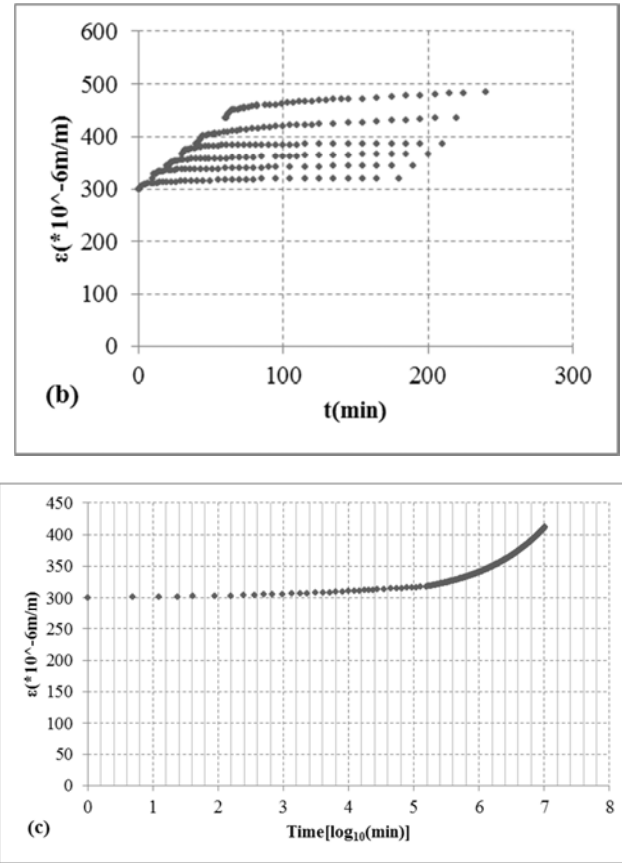
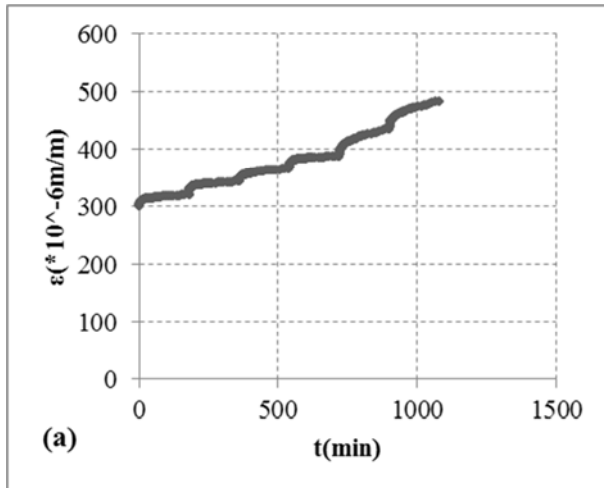


Figure 13. Sequence for SSM data analysis: (a) vertical shifting, (b) rescaling, (c) creep master curve for WW at 5.34% AFS.

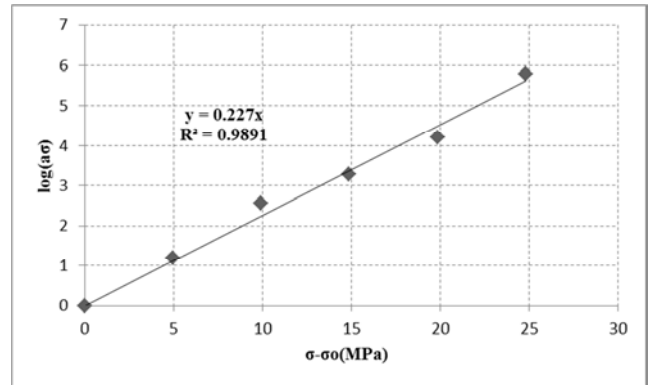


Figure 14. Relationship between stress level and time shift factor.

The master curve of the specimen is included in Figure 13 (c), limited up to two decades. The smoothness and shape of the master curve indicates that the analysis procedure adequately manipulates the data from this testing program to create a realistic creep curve that would result from a conventional long-term test at that reference stress. Furthermore, the relationship between the shift factor and stress level is illustrated in Figure 14. The fact that the data points on this plot lie close to a straight line, with a small experimental scatter, shows that the same creep mechanism is operative for each load sequence, which validates the use of the superposition theory in adding creep curves with different load sequences to produce the creep master curve that

underlies the SSM procedure. From this figure, the activation volume can be described based on the Eyring equation (this model is more suitable for creep behavior of materials at temperatures below the glass transition T_g) [13]:

$$\log_{10}(a_\sigma) = \frac{V^*}{2.30kT}(\sigma - \sigma_0) \quad (8)$$

where $\log_{10}(a_\sigma)$ is the stress-dependent time shift factor, T is absolute temperature (296 K), k is the Boltzmann constant ($1,38 \times 10^{-23} \text{ J.K}^{-1}$), σ_0 and σ are the reference and accelerating stresses (respectively), and V^* is the activation volume. It seems that activation volume is inversely proportional to reference stress. The linear relationship in Figure 14 indicates that the same creep mechanism is likely dominant for the reference stress examined here, meaning the superposition method used in the SSM is valid [16]. For this wood, $V^* = 0,853 \text{ nm}^3$ for 5,34% AFS. There is a relationship between activation volume and stress. According to transition state theory, activation volume V^* for a chemical process is interpreted as the difference between the partial molar volumes of the transition state and the sums of the partial volumes of the reactants at the same temperature and pressure [17]. A physical analogue would be that the products of the creep process occupy a larger volume than the original fiber. This may be consistent with the idea that the molecules are pulled apart during creep. Furthermore, to estimate the creep resistance of the sample under long-term conditions, the modulus reduction (MR) was evaluated using the equation (Equation (6)):

$$MR(\%) = \left[1 - \frac{\varepsilon_0}{\varepsilon(t)} \right] \times 100 \quad (9)$$

where $\varepsilon(t)$ is the time-dependent strain value, ε_0 is the instantaneous elastic strain value, and t is the elapsed time. From this relation, it is clear that since ε_0 is constant and $\varepsilon(t)$ increases with elapsed time, the modulus reduction of the Wengé wood would increase over decades.

4. Conclusion

The main physical and mechanical properties of Wengé determined in this work could be of great interest to engineers when realizing wooden structures with this hardwood. The density was $0,789 \text{ g/cm}^3$, the Young's modulus 21058 MPa. The wood species *Millettia Laurentii* has experienced for the first time the latest accelerated testing method for creep deformation. The so called stepped isostress method has been improved in this work by the means of Maxwell fractional rheological model which allows us to carry up with a higher precision the rescaling step. The main advantage of fractional model being that it takes into account the memory effect of the tested material. It equally contributes to the determination of the activation volume $0,853 \text{ nm}^3$ of the Wengé Wood from Eyring equation. The master curve obtained can be used for predicting the creep

behavior of the test material for time periods more exceeding the experimental one. Since we experienced lower loads in this research work to see how the modified SSM works when applied to Wengé wood materials, the upcoming work will be devoted to the determination of the creep rupture date of the same material under higher stress levels.

Authors' Contributions

All authors contributed equally to the results obtained in this manuscript.

Funding

No fund was reported for this work.

Competing Interests

The authors declare that they have no competing interests.

Acknowledgements

The authors wish to express gratitude to Department of Physics, Mechanics and Modeling of Physical Systems Research Unit for providing the testing facilities.

References

- [1] Patrick Martin; Michel Vernay. Guide d'utilisation des bois africains éco-certifiés. Tome 1. ISBN: 979-10-94-410-01-1.
- [2] Foadieng, E.; Atchounga, K. P.; Talla, P. K. Fractional calculus approach to investigation of creep behavior of Wengé Wood (*Millettia Laurentii*). International Journal of Innovative Science, Engineering & Technology 2019, Vol. 6 Issue 8, 58-68.
- [3] Carneiro, M.; Magalhaes, W.; de Muniz, G.; Schimleck, L. Near infrared spectroscopy and chemometrics for predicting specific gravity and flexural modulus of elasticity of *Pinus* spp. Veneers. J. Infrared Spectrosc 2010a. 18,481. <https://doi.org/10.1255/jnirs.911>.
- [4] Chih-Lung, Cho. Comparison of three methods for determining Young's Modulus of Wood. Taiwan Journal of science 2007. 22 (3): 297-306.
- [5] Tajvidi, M.; Simon, L. C. High-temperature creep behavior of wheat straw isotactic/impact-modified polypropylene composites. J. Thermoplast. Compos. 2015, 28, 1406-1422.
- [6] Hadid, M.; Guerira, B.; Bahri, M.; Zouani, A. Assessment of the stepped isostress method in the prediction of long term creep of thermoplastics. Polym. Test. 2014, 34, 113-119.
- [7] Dasappa, P.; Lee-Sullivan, P.; Xiao, X. Temperature effects on creep behavior of continuous fiber GMT composites. Compos. Part A 2009, 40, 1071-1081.
- [8] Jones, C. J. F. P.; Clarke, D. The residual strength of geosynthetic reinforcement subjected to accelerated creep testing and simulated seismic events. Geotext. Geomembr. 2007, 25, 155-169.

- [9] Alwis, K. G. N. C.; Burgoyne, C. J. Accelerated creep testing for aramid fibres using the stepped isothermal method. *J. Mater. Sci.* 2008, 43, 4789–4800.
- [10] Yeo, S. S.; Hsuan, Y. G. Evaluation of creep behavior of high density polyethylene and polyethylene-terephthalate geogrids. *Geotext. Geomembr.* 2010, 28, 409–421.
- [11] Achereiner, F.; Engelsing, K.; Bastian, M.; Heidemeyer, P. Accelerated creep testing of polymers using the stepped isothermal method. *Polym. Test.* 2013, 32, 447–454.
- [12] Hadid, M.; Rechak, S.; Tati, A. Long-term bending creep behavior prediction of injection molded composite using stress-time correspondence principle. *Mater. Sci. Eng. A Struct.* 2004, 385, 54–58.
- [13] Giannopoulos, I. P.; Burgoyne, C. J. Prediction of the long-term behaviour of high modulus fibres using the stepped isostress method (SSM). *J. Mater. Sci.* 2011, 46, 7660–7671.
- [14] Giannopoulos, I. P.; Burgoyne, C. J. Accelerated and real-time creep and creep-rupture results for aramid fibers. *J. Appl. Polym. Sci.* 2012, 125, 3856–3870.
- [15] Schapery, R. A. On the characterization of nonlinear viscoelastic materials. *Polym Eng Sci* 1969; 9 (4): 295–310.
- [16] Yang, T. C.; Wu, T. L.; Hung, K. C.; Chen, Y. L.; Wu, J. H. Mechanical properties and extended creep behavior of bamboo fiber reinforced recycled poly (lactic acid) composites using the time-temperature superposition principle. *Constr. Build. Master.* 2015, 93, 558–563.
- [17] Truhlar, D. G.; Garrett, B. C.; Klippenstein, S. J. *J Phys Chem.* 1996, 100 (31): 12771.